

Available online at www.sciencedirect.com

ScienceDirect

journal homepage: www.elsevier.com/locate/jasi

Original Article

Cochleotomy of human cochlear nucleus

S. Sharma ^a, B. Ray ^b, A.K. Dinda ^c, T.S. Roy ^{d,*}^a Assistant Professor, M.D, PhD, Department of Anatomy, Vardhaman Mahavir Medical College and Safdarjung Hospital, New Delhi 110029, India^b Assistant Professor, MD, Department of Neurology, University of Oklahoma College of Medicine, Oklahoma City, USA^c Professor, PhD, Department of Pathology, All India Institute of Medical Sciences, Ansari Nagar, New Delhi 110029, India^d Professor and Head, M.D, PhD, Department of Anatomy, All India Institute of Medical Sciences, Ansari Nagar, New Delhi 110029, India

ARTICLE INFO

Article history:

Received 11 November 2014

Accepted 1 April 2015

Available online 18 April 2015

Keywords:

Auditory nerve and spiral ganglion

Cochlear nucleus

Synaptophysin

MAP-2

Ca-binding proteins

ABSTRACT

Introduction: The human peripheral auditory pathway in infants is a relatively less explored domain in auditory research. In the present study, the cochlea, auditory nerve (AN) and the cochlear nucleus (CN) were examined using immunohistochemistry and light and electron-microscopy.

Methods: The study was performed on specimens retrieved from a 40-day-old infant who could not survive after corrective surgery for congenital cyanotic heart disease. The donation was done in accordance with the protocol approved by the Human Ethics Committee, All India Institute of Medical Sciences (AIIMS), New Delhi, India.

Results: The AN revealed degeneration of nerve fascicles originating from the spiral ganglion neurons of the middle and basal turns of the cochlea. The proximal and middle segments of the nerve showed varying degrees of degenerating fibers with macrophages whereas the most distal part of the nerve showed dilated endoneurial capillaries without any degeneration. On electron-microscopy, the nerve revealed features of acute myelinopathy. The differential perisomatic synaptophysin immunoreactivity was observed in the CN. The unaffected neurons showed strong microtubule-associated protein 2 (MAP-2) immunoreactivity, while those denervated revealed decreased staining. The VCN showed varying degree of parvalbumin (PV) and calbindin (CB) immunostaining with AN fibers and terminals showing strong immunoreactivity for PV. The AN revealed strong immunoreactivity for CB on the affected side. The spiral ganglion neurons did not reveal any pathological changes.

Discussion: The results provide a cochleotopic map of the human CN that maybe relevant in better understanding of the tonotopic organization and will be helpful during auditory implants in children.

Copyright © 2015, Anatomical Society of India. Published by Reed Elsevier India Pvt. Ltd. All rights reserved.

* Corresponding author. Department of Anatomy, All India Institute of Medical Sciences, Ansari Nagar, Room 1018, New Delhi 110029, India. Tel.: +91 11 26594880, +91 11 26593216; fax: +91 11 26588663.

E-mail addresses: tarasankar@hotmail.com, tsroy@aiims.ac.in (T.S. Roy).

<http://dx.doi.org/10.1016/j.jasi.2015.04.001>

0003-2778/Copyright © 2015, Anatomical Society of India. Published by Reed Elsevier India Pvt. Ltd. All rights reserved.

1. Introduction

Post-operative sensorineural hearing loss (SNHL) after cardiopulmonary bypass surgery, though rare is a well-documented complication in elderly patients undergoing such procedure during coronary artery bypass graft surgery.¹ SNHL in these post-operative cases is usually diagnosed using audiometric parameters.² Pathological involvement of the peripheral organ of hearing simultaneously affect brainstem cochlear nucleus (CN), which is the first relay station of the auditory pathway and leads to alterations in physiology, metabolism and morphology in the CN.³ The temporary loss of sensory impulses lead to transient increase in the calcium binding proteins (CaBP – calbindin and parvalbumin) to buffer the toxic effects of increased calcium ions (Ca²⁺).⁴ Synaptophysin (SYN) is a 38-kDa protein present in the membranes of the central synaptic vesicles and its expression provides an indirect measure of synaptic activity.⁵ Similarly, microtubule-associated protein 2 (MAP-2) is a cytoskeleton protein, predominantly localized in the cell body and the dendrites of neurons, which is down-regulated during auditory deprivation.⁶

As a continuation of our previous study⁷ on human auditory nerve (AN) we encountered a degenerating AN on the right side of a forty-day old female infant. The infant had undergone corrective procedure for congenital cyanotic heart disease and expired during the post-operative period. Since the cochlea and brainstem were also preserved during tissue collection, we had the rare opportunity to study the peripheral and central targets of the AN. In our previous works on human fetal cochlear nerve⁷ and CN, the expression of SYN, MAP-2, parvalbumin (PV) and calbindin (CB) was observed.^{8,9} Hence, in the present study, we had the unique opportunity to compare pathological pattern of expression of above-mentioned proteins in brainstem as compared to previously documented normal pattern and thus attempt to establish cochleotopic representation of the CN. The site and nature of involvement were also assessed using light and electron-microscopy. In the present study we also attempt to lay emphasis on the clinical relevance of the observed auditory pathology.

2. Materials and methods

2.1. Subject

The present study was performed on the tissues obtained from the donated body (40-day old female infant) that died due to post-operative complication following cardiac surgery. The donation was done by the parent of the deceased for research and teaching purpose in accordance with the protocol approved by the Human Ethics Committee, All India Institute of Medical Sciences (AIIMS), New Delhi, India under the guidelines of Helsinki declaration. The clinical, operative and post-operative findings were noted from the Medical Records Section, AIIMS, New Delhi, India.

The patient was hospitalized with fever, difficulty in breathing and poor weight gain. The baby was a normal full

term delivery with no perinatal hypoxia and uneventful prenatal history. The patient was alert with good cry, but revealed mild cyanosis and a systolic murmur at the cardiac apex. The chest x-ray showed right ventricular apex with right arch and dilated right atrium and ventricle. The diagnosis of Type I truncus arteriosus was confirmed on echocardiography with color Doppler and angiography. There was small patent foramen ovale, large ventricular septal defect with 70% overriding of the great arteries and hypoplastic left pulmonary artery. The laboratory parameters were within normal limits. The corrective operation was uneventful and arterial blood gases and electrolytes were maintained during the operative and early post-operative period. There was a sudden drop in these parameters about 4 h (h) after the operation and the patient could not be revived by resuscitative measures.

2.2. Tissue fixation and sample retrieval

The deceased infant was embalmed through the ascending aorta using 4% paraformaldehyde (PF) (in 0.1 M phosphate buffer (PB), pH 7.4). Craniotomy was performed to remove the brain and transferred to freshly prepare 4% PF (with a change of fresh fixative after 48 h). The brainstem was separated, sectioned in two halves and kept in 4% PF for 1 week at 4 °C. The AN on both sides were exposed under the Ultrascope MK II (Optech International Ltd., New Zealand), by de-roofing the temporal bone in the internal acoustic meatus region containing the bony cochlea. The entire nerve from the base to brainstem was retrieved and placed in freshly prepared Karnovsky's fixative (1% glutaraldehyde, 4% PF in 0.1 M PB) with a change of fresh fixative after 6 h and kept for 24 h and then transferred to 0.1 M PB till further processing. The cochlea of the right side was dissected out and transferred to Karnovsky's fixative for 48 h.

2.3. Brainstem processing for light microscopy and immunohistochemistry

Each half of the brainstem was rinsed in PB, cryoprotected in 30% sucrose and transverse frozen sections (14–16 µm) were cut and mounted on gelatin coated slides. For Nissl staining, sections were dehydrated in ascending concentration of alcohol, stained with 1% cresyl violet (CV), mounted and viewed and photographed under Zeiss Axiophot Research Microscope (Germany).

2.3.1. Immunohistochemistry

The sections were treated in 0.3% hydrogen peroxide in 80% methanol for 1 h to quench the endogenous peroxidase activity and then washed in 80% methanol, 50% methanol, 0.1M PB and 0.01M PBSTx. After washing, the sections were incubated in 10% normal horse serum in 0.01 M PB saline containing 0.5% Triton-X-100 (PBSTx) for 2 h. The sections were then incubated in the monoclonal primary antisera against SYN (1:100; Boehringer Mannheim Biochemica, Germany), MAP-2 (1:1000; Pierce Biotechnology Inc. USA), PV (1:1000; Sigma Chemicals Co., USA) and CB (1:1000; Sigma Chemicals Co., USA) for 48 h at 4 °C. The sections were washed with 0.01M PBSTx and incubated in biotinylated anti-mouse

secondary antibody (Vector Laboratories, Burlingame, CA, USA) for 5–6 h at 4 °C. This was followed by avidin-biotin peroxidase complex (Vector Laboratories, Burlingame, CA, USA) incubation for 2 h and the binding sites of antigen–antibody interactions were visualized by using 0.06% diaminobenzidine tetrahydrochloride as chromogen and 0.06% hydrogen peroxide in 0.01 M acetate-imidazole buffer (pH 7.4). The sections were washed, dehydrated and mounted in DPX. For negative control staining, all steps were followed except the primary antibody step.

2.4. Tissue processing for light and electron microscopy

2.4.1. Auditory nerve

The specimens were postfixed in 1% osmium tetroxide (in 0.1M PB) for 2 h, washed, dehydrated in ascending grades of acetone, embedded and blocked in araldite. The cochlear end of the nerve, where the fibers from the spiral ganglion join to form the AN was kept as the cutting surface. Semi-thin (1 µm) cross-sections of the nerve were cut with glass knife on a Reichert Ultramicrotome, stained with 1% toluidine blue and mounted. Ultrathin sections (~50–60 nm) of the nerves were picked up randomly on 300-mesh copper grids, stained with uranyl acetate/lead citrate protocol and viewed under a Philips Morgagni 268 transmission electron microscope (TEM).

2.4.2. Cochlea

After fixation, the cochlea was rinsed in 0.1 M PB, decalcified using 10% EDTA solution for 2 weeks and the end point of decalcification was checked using X-ray. The cochlea was then bisected at the modiolus and then further cut perpendicular to the modiolus. The resin embedding protocol was followed as described above and the modiolar surface was kept as the cutting surface.

3. Results

3.1. Cochlear nucleus

The CN and its subdivisions; ventral and dorsal (VCN and DCN) were seen lateral to the inferior cerebellar peduncle (ICP) using CV stained sections (Fig. 1a). The different types of neurons in the VCN and DCN were identified as described in our previous paper.¹⁰ None of the neurons observed in the VCN and DCN revealed any gross evidence of chromatolysis or cell swelling.

3.1.1. Immunohistochemistry

3.1.1.1. SYN expression. SYN immunoreactivity was examined to assess the morphologic evidence of synaptic integrity of the CN. The neurons located ventral, ventromedial and

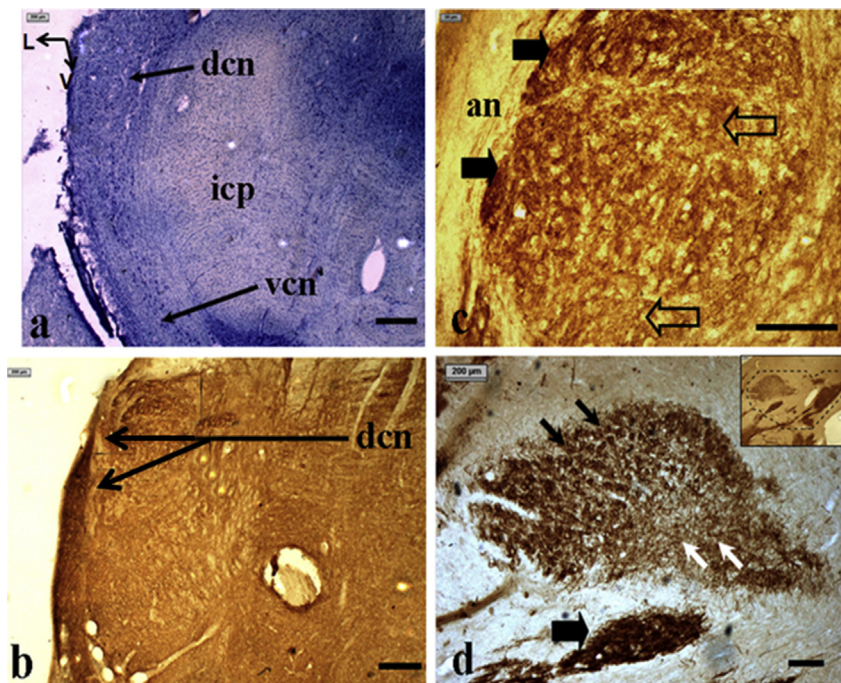


Fig. 1 – Photomicrograph of Nissl staining and synaptophysin expression in the human cochlear nucleus of 40 day infant. (a) Cresyl violet stained transverse section of brainstem. Dorsal and ventral cochlear nucleus (dcn and vcn) lateral to the inferior cerebellar peduncle (icp), rotated orientation arrows indicating the ventral (V) and lateral (L). (b) Synaptophysin immunoreactivity in the dorsal cochlear nucleus (dcn). (c) At higher magnification mostly perisomatic expression seen in the DCN neurons. Note the high intensity of immunoreactivity (block arrows) as compared to less immunostaining (open arrows). Note the unstained auditory nerve (an) fibers. (d) Photomicrograph of cranial VCN shows strong immunoreactivity in the medial part (block arrow); perisomatic staining of moderate intensity in the dorsolateral aspects (black arrows) and diffuse punctate immunostaining in ventrolateral region (white arrows). Inset shows low magnification view of VCN complex (dotted area). Scale bar – a, b, d-200 µm; c-50 µm.

dorsomedial aspect of the CN on the affected side (right – R) revealed predominantly perisomatic immunoreactivity while those on the lateral aspect had a more punctuate staining (Fig. 1b, c and d). The AN fibers were SYN negative (Fig. 1c).

3.1.1.2. MAP- 2 expression. MAP-2 immunoreactivity was examined to assess the cytoskeletal integrity of the neurons in the CN. On the affected side (R), neurons near the auditory nerve root were strongly positive for MAP-2 (Fig. 2a and b) whereas the major part of the VCN showed weak to moderate diffuse immunoreactivity for MAP-2 (Fig. 2c). Distinct punctate appearance immunostaining in the neuronal bodies was seen on the unaffected side (left- L). The DCN revealed weak to moderate immunoreactivity to MAP-2.

3.1.1.3. PV and CB expression. PV and CB immunoreactivity was examined to assess the calcium buffering capacity of the CN neurons. In the VCN, the cell density of PV positive neurons was more on the affected side (R) (Fig. 3b and d) as compared to the unaffected side (L) (Fig. 3a and c). The differential CB expression was seen in the VCN (Fig. 3e and f). The AN fibers were strongly positive for PV and CB on the affected

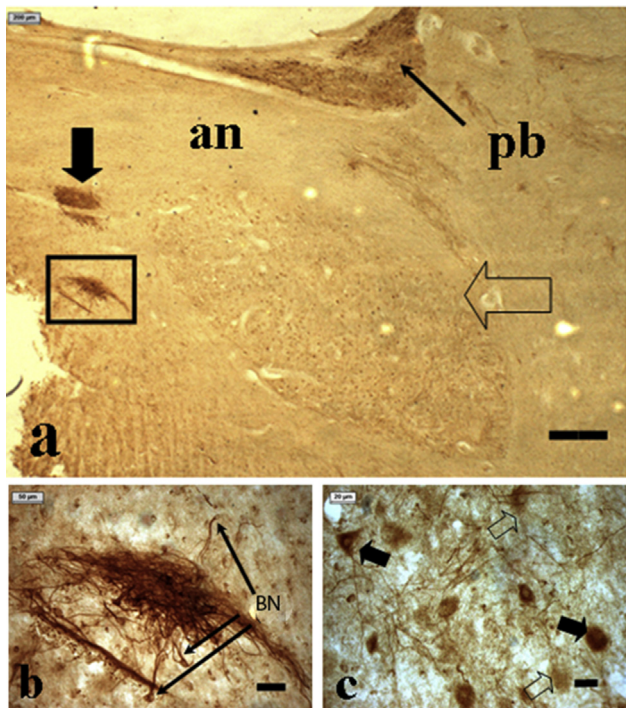


Fig. 2 – Photomicrograph of MAP-2 expression in the affected human VCN. (a) High MAP-2 expression in the neurons (block arrow and framed area) near the auditory nerve root (an), low to moderate expression in major part of the VCN (open arrow). MAP-2 expression in the neurons of the pontobulbar body (pb). (b) The boxed area in (a) at a higher magnification showing MAP-2 immunostained bushy neurons (BN) and dendrites (Black arrows). (c) Photomicrograph showing moderate (block arrows) and weak (open arrows) MAP-2 expression in the VCN neurons. Scale bar: a – 400 μ m, b – 50 μ m; c – 20 μ m.

side (R) (Fig. 3b and f) as compared to weak to moderate staining on the unaffected side (L) (Fig. 3a and e).

3.2. Auditory nerve

3.2.1. Light microscopy

Toluidine blue stained semithin sections at various levels of the AN were examined for neural and connective tissue organization. On the affected side (R) the distal end of the nerve showed well organized fascicles with no evidence of degeneration. Groups of small fascicles from the lower basilar turn of the cochlea were seen joining fibers from the preceding regions of the cochlea (Fig. 4a). Very few endoneurial blood vessels were dilated along with normal endoneurial blood vessels (Fig. 4b). We also observed few spiral ganglion neurons among the nerve fibers (Fig. 4b). At the mid portion of the AN, the fascicles having fibers from lower middle turn and basal turns of the cochlea showed features of degeneration (Fig. 4c and d). The severely affected axons showed disruption of both the axon profile as well as the myelin. The macrophages having a foamy cytoplasm indicated the presence of inflammation (Fig. 4d). The proximal end of the AN showed thinly myelinated nerve fibers and lack of small fascicular arrangement, though three fascicles (large, medium and small) were observed (Fig. 4e). The AN on the unaffected side (L) did not show any feature of degeneration (Fig. 4f). The spiral ganglion neurons were identified in groups in the Rosenthal's canal (Fig. 4g) in toluidine blue stained semithin sections. No inflammatory cells or feature of degeneration was observed in the AN fibers (an) emerging from the middle turn. The neurons in the middle turn were closely positioned to each other as compared to the basal turn (Fig. 4h).

3.2.2. Electron microscopy

The ultrastructural features corroborated with the light microscopic observations. The unaffected portion of the nerve did not reveal any feature of degeneration (Fig. 5a and c). There was distinct feature of degenerating myelin and axons dispersed among macrophages and microglia in the pathological portion (Fig. 5b). The glycogen granules were observed both inside the macrophages and microglia in the peripheral and central part of the AN respectively (Fig. 5d).

4. Discussion

Our present study describes the possible cochleotopic arrangement of the cytoarchitectural organization of the AN fibers and spiral ganglion and CN neurons and the differential expression of SYN, MAP-2, PV and CB in pathological brainstem. This is the first time such cochleotopy is being reported in human infant. Given the rarity and difficulty in obtaining such specimens, this study objectively describes cochleotopy of CN in human despite being on a single specimen.

4.1. Cochlear nuclear cochleotopy

The pattern of expression of SYN in the CN demonstrates a probable cochleotopic innervation. However, to what extent the SYN expression is regulated under pathological

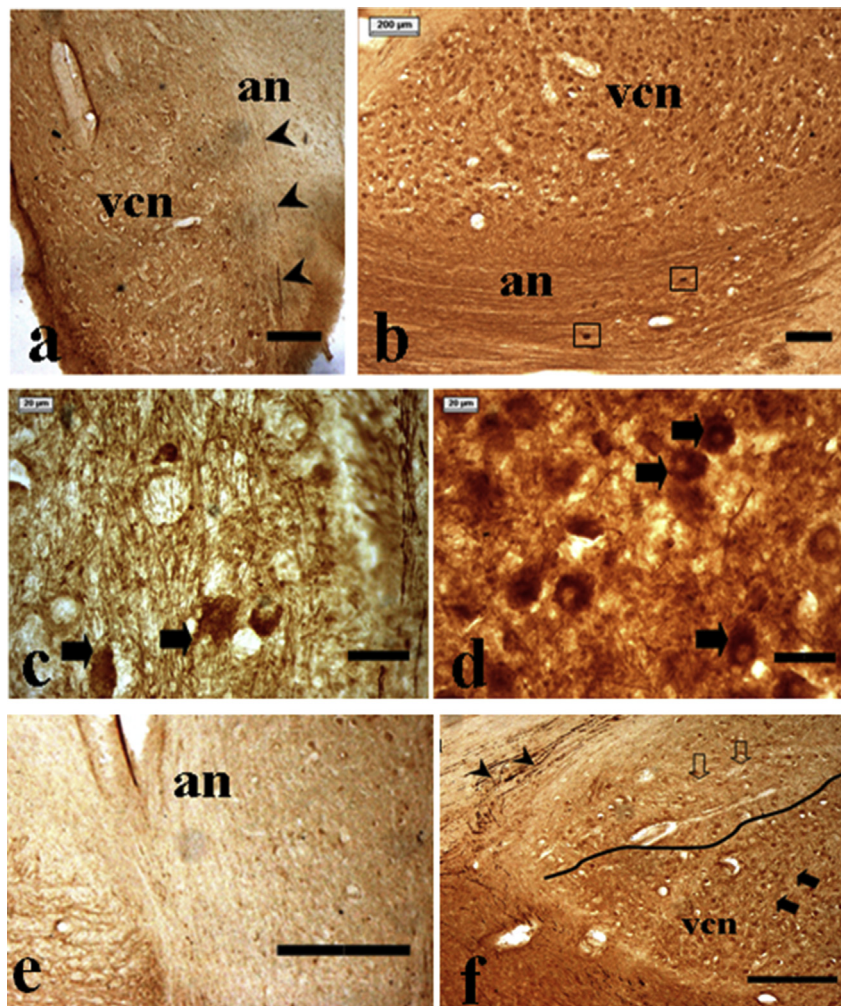


Fig. 3 – Photomicrographs of Parvalbumin and Calbindin expression in the human VCN. PV stained sections of brainstem showing VCN on unaffected (Left) (a) and affected (Right) (b) sides. At higher magnification, note the weak expression of PV positive neurons on the unaffected side (c) whereas increased density of PV positive neurons (block arrows) on the affected side (d). CB stained sections of brainstem showing VCN on the unaffected (e) and affected (f) sides. Note the increased density of CB positive neurons on the lateral side (block arrows) of the VCN compared to few on its medial side (open arrows). Approximate demarcation between the two areas is depicted by the black line. Most of the AN fibers (an) are strongly immunoreactive to PV and CB on the affected side (b and f) as compared to only few immunoreactive fibers on the unaffected side (a and e: arrowheads). Scale bar: a, b – 200 μm ; c, d – 40 μm ; e, f – 400 μm .

conditions in the central nervous system is not known.¹¹ The decreased immunostaining and loss of perisomatic distribution of the terminals on the lateral and dorsolateral aspect of the CN probably reflects the predominant representation of the basal fibers in these regions. This may be due to true denervation of the affected region or a transient down-regulation of SYN expression due to the pathology in the AN but needs further in-depth study. Similar loss of perisomatic terminals are also seen in animal models of denervation.⁵ MAP-2 expression in human fetal and adult auditory brainstem nuclei was studied and the dendritic distribution of the neurons without cytoarchitectural organization of the CN is described.¹² The dendrogenesis was seen even in post natal period and is important for neuronal activity. The presence of diffuse differential MAP-2 immunoperoxidation in the present case may affect the neuronal

activity¹² and also play a role in deafferentation-induced dendritic remodeling.¹³

The increase in the density of PV and CB positive neurons on the affected side (R) probably indicates the up-regulation of these buffering proteins in the VCN. The PV expression shows a more diffuse distribution in the affected CN (R). The up-regulation of CaBP was also observed in the AN fibers entering the CN. PV is expressed in most of the fibers on the affected side (R) while only few fibers over-expressed CB. Similar over-expression of the CaBP in the CN was also observed in animal models of cochlear ablation using glutamate agonist to transiently denervated inner hair cells from primary auditory dendrites.⁴

The AN arising from the spiral ganglion neurons is entering the CN and bifurcate into ascending and descending branches (root branch).¹⁴ It is suggested that the length of the root

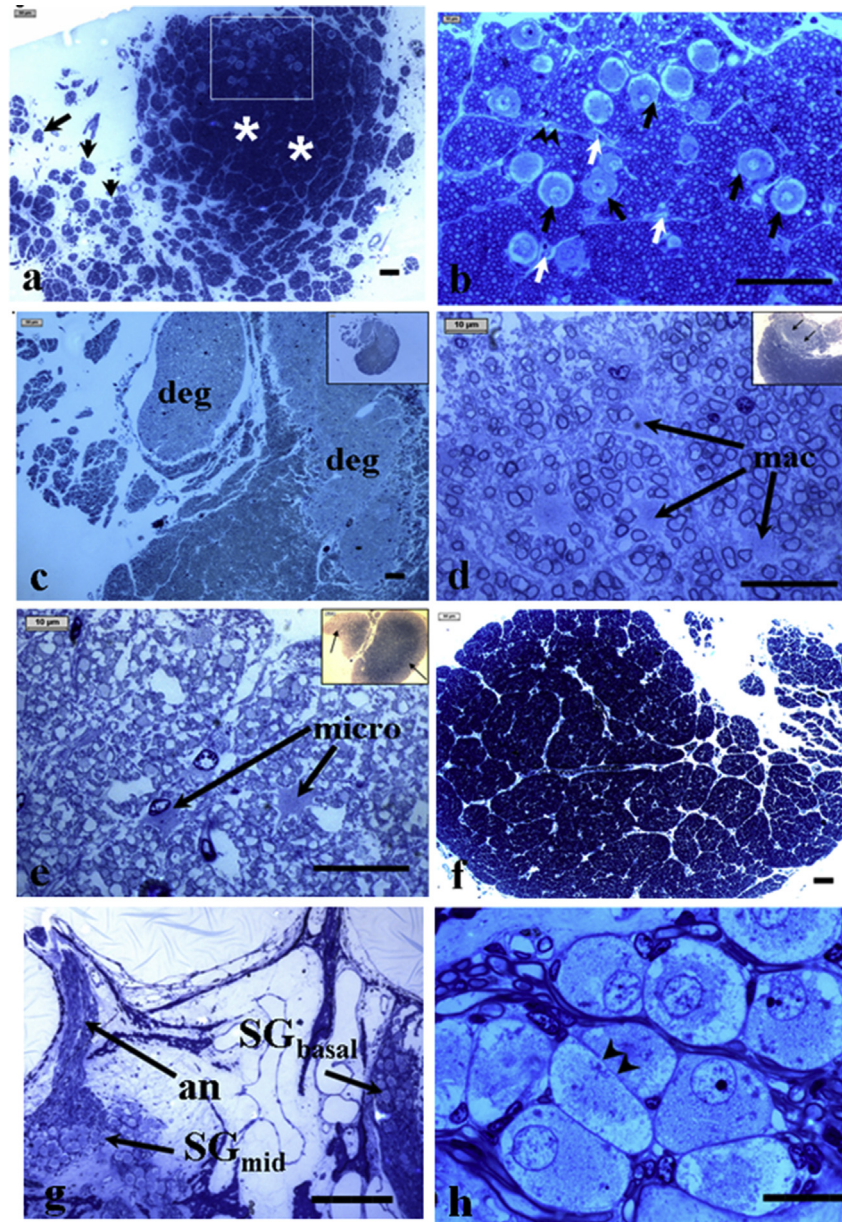


Fig. 4 – Photomicrograph of Auditory nerve (AN) at various levels. (a) Distal portion of the AN showing nerve fascicles from the basal parts of the cochlea (arrows) joining with the fibers from the middle and apical parts (white star: *). Note few spiral ganglion neurons (SGN in boxed area). **(b)** The boxed area in (a) at a higher magnification showing few endoneurial dilated capillaries as compared to the rest of the endoneurial capillaries (white arrows). Intact perineurial cells (arrowheads) indicate maintenance of blood-nerve-barrier. Few SGN were observed (black arrows) **(c)** Mid-portion of the AN showing the features of degeneration (deg; light stained area). Inset: Entire profile of the nerve. **(d)** Section of the nerve at a more proximal site showing endoneurial macrophages (mac). Note faintly stained portion of the basal fibers (small arrows) (Inset). **(e)** Proximal (central) portion of the AN showing indistinct fascicular arrangement, thin myelin sheath and few microglia (micro). Inset shows the entire nerve section which reveals degeneration only in the peripheral part of the AN (arrows). **(f)** AN on the unaffected side (left) shows no degenerating fascicles. **(g)** Photomicrograph of the cochlea shows SGN in the middle and basal turns (SG_{mid} and SG_{basal}) on the affected side (right). **(h)** SGN at higher magnification showing membrane contacts (arrowheads) between spiral ganglion neurons in the middle turn. Scale bar: a, b, c, f – 50 μm ; d, e – 25 μm ; g – 200 μm ; h – 20 μm .

branch is same irrespective of the origin of the fiber, from the base or the apex.^{14–16} Thus the fibers arising from the apex are represented ventrally while those from the base have a dorsal representation.^{17–20} We also observed few spiral ganglion

neurons in the AN fibers which needs further in-depth study to make a decision on their origin. Our results on the human CN also showed similar cochleotopic organization with ventromedial representation of fibers coming from apical

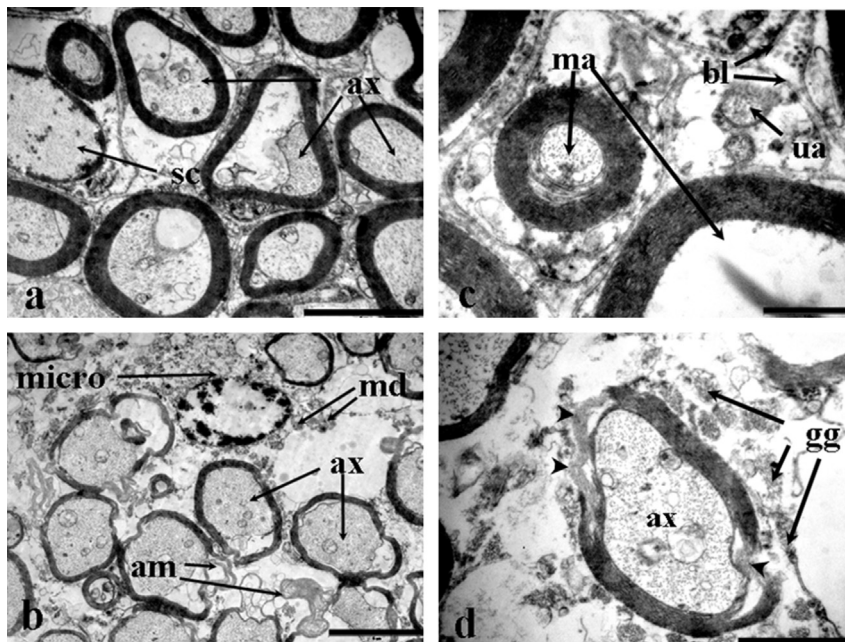


Fig. 5 – Electronmicrographs of the affected AN (right). (a) Unaffected portion of the distal AN showing axons (ax) having intact myelin sheaths. A Schwann cell (sc) is seen wrapping a myelinated axon. (b) Activated microglia (micro) containing myelin debris (md) was seen in the affected portion of the proximal AN. Abnormal myelin (am) sheaths surround the apparently normal axons (ax). (c) The unaffected portion of the distal part of AN showing intact myelinated and unmyelinated axons (ma and ua respectively) with intact basal lamina (bl). (d) The affected portion of the distal part of AN showing patchy myelin loss (arrowheads) from the axon (ax). Glycogen granules (gg) are seen in the cytoplasm of the Schwann cells. Scale bar: a, b – 5 μ m; c – 1 μ m; d – 2 μ m.

cochlea. The probable short duration of the pathological insult occurring within four hours of the post-operative period did not allow complete denervation effect to develop in the CN. But the initial down-regulation of SYN, MAP-2 and up-regulation of CaBP provide a “place” map of cochleotopic innervation of the CN.

4.2. Auditory nerve pathology

The incidence of auditory neuropathy has been estimated to be 10.3% in the pediatric population²¹ which is contributed by various causes.²² The pathology may be in the AN proper or synaptic abnormality with the hair cell or CN. The pathology observed in the present case involved segmental demyelination of the proximal part of the AN as evidenced by the presence of degenerating fibers and macrophages. These changes in the proximal part may be located around the transitional zone of the nerve having high metabolic activity due to the presence of nodal regions of the nerve fibers.²³ Hence, it might be postulated that in the present case there might had been an insult compromising the vascularity of the critical region resulting in hypoxia and activation of macrophages. The resident endoneurial macrophages (REM) are probably responsible for the present pathology as evidenced by absence of hematogenous macrophages within the intact endoneurial capillaries in the severely affected portions of the nerve. Though we admit that in human nerve biopsies, differentiation between

resident and infiltrating endoneurial macrophages is essentially impossible using electron-microscopic techniques.²⁴ The REM is activated as early as two days of crush injury in the sciatic nerve with infiltration of hematogenous macrophages occurring from the fourth day.²⁵ Considering the injury to be intra-operative the activation of the REM fails to explain the pathology seen in the present case. But REM may be activated even earlier in response to an auto-immune insult²⁴ or ischemic insult. Since, the patient had congenital cyanotic heart disease we are unsure if chronic hypoxemia might have played any role in this predisposition. Moreover, microglial cells are activated early in response to any kind of central nervous system injury.²⁶ Hence, it may well be speculated that the probable injury at the transitional zone of the AN may lead to rapid activation of the microglia from which putative cytokines diffused into the peripheral portion and led to activation REM.

4.3. Clinical implications

In the present case since the auditory neuropathy is restricted to one side with normal morphology of the AN on the contralateral side, there should not be apparent difficulty in hearing. But since the pathological AN contains both normal and demyelinated axons, slow conduction in the involved fibers is expected which may lead to auditory dys-synchrony. Synchronization of neural discharges is

required for correct encoding of auditory percepts like loudness, pitch and temporal fine structure.²² Temporal fine structure is critical in deciphering complex sound features and enabling speech perception. The subject in the present study, being prelingual would have difficulty in learning languages with defect in speech perception. It is reported that electric stimulation of spiral ganglion neurons through cochlear implants could provide reliable and consistent nerve conduction even in the presence of a diseased AN.²⁷ Some authors even propose that electric stimulation may even facilitate neural survival and restore temporal encoding.²⁸

There are reports of nerve survival and better electrical stimulation after implantation of penetrating electrodes in the CN in experimental animals.^{29–31} It will be necessary to assess the feasibility, complications, neuronal survival and continued stimulation before a penetrating ABI is clinically available.³²

5. Conclusion

We report the morphology and immunoexpression of SYN, MAP-2 and CaBP in the human AN, spiral ganglion neurons and CN in a post-operative case of Type 1 Truncus arteriosus in a 40- day infant. Our results describing cochleotopy of CN adds new information and further contribute in facilitating the development of new age auditory prosthesis to re-establish the hearing and social rehabilitation in case of hearing loss.

Conflicts of interest

All authors have none to declare.

Acknowledgments

We acknowledge the contribution of Head and Prof. Shashi Wadhwa from department of Anatomy, North Delhi Municipal Corporation Medical College at Bara Hindu Rao hospital Malkagang, Delhi. We immensely acknowledge the contribution parents of the deceased who donated the infant's body for research and teaching.

REFERENCES

1. Arenberg IK, Allen GW, DeBoer A. Sudden deafness immediately following cardiopulmonary bypass. *J Laryngol Otol.* 1972;86:73–77.
2. Young IM, Mehta GK, Lowry LD. Unilateral sudden hearing loss with complete recovery following cardiopulmonary bypass surgery. *Yonsei Med J.* 1987;28:152–156.
3. Rubel EW, Hyson RL, Durham D. Afferent regulation of neurons in the brain stem auditory system. *J Neurobiol.* 1990;21:169–196.
4. Caicedo A, d'Aldin C, Eybalin M, et al. Temporary sensory deprivation changes calcium-binding proteins levels in the auditory brainstem. *J Comp Neurol.* 1997;378:1–15.
5. Muly SM, Gross JS, Morest DK. Synaptophysin in the cochlear nucleus following acoustic trauma. *Exp Neurol.* 2002;177:202–221.
6. Kelley MS, Lurie DI, Rubel EW. Rapid regulation of cytoskeletal proteins and their mRNAs following afferent deprivation in the avian cochlear nucleus. *J Comp Neurol.* 1997;389:469–483.
7. Ray B, Roy TS, Wadhwa S, et al. Development of the human fetal cochlear nerve: a morphometric study. *Hear Res.* 2005;202:74–86.
8. Mishra S. *Morphological and Neurochemical Study of Human Cochlea and Cochlear Nuclei in Prenatal Period.* PhD thesis. New Delhi, India: All India Institute of Medical Sciences; 2001.
9. Sharma S, Nag TC, Thakar A, et al. The aging human cochlear nucleus: changes in the glial fibrillary acidic proteins, intracellular calcium regulatory proteins, GABAergic neurotransmitter and cholinergic receptors. *J Chem Neuroanat.* 2014;56:1–12.
10. Sharma S, Nag TC, Thakar A, et al. Age associated changes in the human cochlear nucleus - a three-dimensional modelling and its potential application for brainstem implants. *J Anat Soc India.* 2014;63:12–18.
11. Hannah MJ, Schmidt AA, Huttner WB. Synaptic vesicle biogenesis. *Annu Rev Cell Dev Biol.* 1999;15:733–798.
12. Moore JK, Guan YL, Shi SR. MAP2 expression in developing dendrites of human brainstem auditory neurons. *J Chem Neuroanat.* 1998;16:1–15.
13. Wang Y, Rubel EW. Rapid regulation of microtubule-associated protein 2 in dendrites of nucleus laminaris of the chick following deprivation of afferent activity. *Neuroscience.* 2008;154:381–389.
14. Arnesen AR, Osen KK. The cochlear nerve in the cat: topography, cochleotopy, and fiber spectrum. *J Comp Neurol.* 1978;178:661–678.
15. Fekete DM, Rouiller EM, Liberman MC, et al. The central projections of intracellularly labeled auditory nerve fibers in cats. *J Comp Neurol.* 1984;229:432–450.
16. Ryugo DK. The auditory nerve: peripheral innervation, cell body morphology and central projections. In: Webster DB, Popper AN, Fay RR, eds. *Springer Handbook of Auditory Research, The Mammalian Auditory Pathway: Neuroanatomy.* vol. 1. New York: Springer-Verlag; 1992:23–65.
17. Osen KK. Course and termination of the primary afferents in the cochlear nuclei of the cat. An experimental anatomical study. *Arch Ital Biol.* 1970;108:21–51.
18. Webster DB. Projection of the cochlea to cochlear nuclei in Merriam's kangaroo rat. *J Comp Neurol.* 1971;143:323–340.
19. Ryugo DK, Rouiller EM. Central projections of intracellularly labeled auditory nerve fibers in cats: morphometric correlations with physiological properties. *J Comp Neurol.* 1988;271:130–142.
20. Leake PA, Snyder RL. Topographic organization of the central projections of the spiral ganglion in cats. *J Comp Neurol.* 1989;281:612–629.
21. Sininger YS. Identification of auditory neuropathy in infants and children. *Semin Hear.* 2005;23:193–200.
22. Tibesar RJ, Shallop JK. Auditory neuropathy. In: Cummings CW, ed. *Otolaryngology, Head and Neck Surgery.* 4 ed. vol. 4. Philadelphia: Elsevier & Mosby; 2005:3503–3521.
23. Berthold CH, Fraher JP, King RHM, et al. Microscopic anatomy of the peripheral nervous system. In: Dyck PJ, Thomas PK, eds. *Peripheral Neuropathy.* 4 ed. Philadelphia: Elsevier & Saunders; 2005:35–91.

24. Kiefer R, Kieseier BC, Stoll G, et al. The role of macrophages in immune-mediated damage to the peripheral nervous system. *Prog Neurobiol.* 2001;64:109–127.
25. Mueller M, Wacker K, Ringelstein EB, et al. Rapid response of identified resident endoneurial macrophages to nerve injury. *Am J Pathol.* 2001;159:2187–2197.
26. Kreutzberg GW. Microglia: a sensor for pathological events in the CNS. *Trends Neurosci.* 1996;19:312–318.
27. Zhou R, Abbas PJ, Assouline JG. Electrically evoked auditory brainstem response in peripherally myelin-deficient mice. *Hear Res.* 1995;88:98–106.
28. Shannon RV, Zeng FG, Kamath V, et al. Speech recognition with primarily temporal cues. *Science.* 1995; 270:303–304.
29. Rosahl SK, Mark G, Herzog M, et al. Far-field responses to stimulation of the cochlear nucleus by microsurgically placed penetrating and surface electrodes in the cat. *J Neurosurg.* 2001;95:845–852.
30. Badi AN, Hillman T, Shelton C, et al. A technique for implantation of a 3-dimensional penetrating electrode array in the modiolar nerve of cats and humans. *Arch Otolaryngol Head Neck Surg.* 2002;128:1019–1025.
31. Badi AN, Kertesz TR, Gurgel RK, et al. Development of a novel eighth-nerve intraneural auditory neuroprosthesis. *Laryngoscope.* 2003;113:833–842.
32. Gantz BJ, Meyer TA. Auditory brainstem implantation. In: Cummings CW, ed. *Otolaryngology, Head and Neck Surgery.* 4 ed. vol. 4. Philadelphia: Elsevier & Mosby; 2005:3845–3854.